

Supplementary Information

Laboratory Protocols for Measuring and Reporting the Performance of Luminescent Solar Concentrators

Michael G. Debije^{1*}, Rachel C. Evans^{2*}, Gianmarco Griffini^{3*}

¹Department of Chemical Engineering and Chemistry, Eindhoven University of Technology (Netherlands)

*e-mail: m.g.debije@tue.nl

²Department of Materials Science & Metallurgy, University of Cambridge (United Kingdom)

*e-mail: rce26@cam.ac.uk

³Department of Chemistry, Materials and Chemical Engineering “Giulio Natta”, Politecnico di Milano (Italy)

*e-mail: gianmarco.griffini@polimi.it

Table of Contents

1. LSC device parameters and optical losses
2. Example calculations of key LSC metrics

Supporting data files available for example calculations:

Data_absorbance.txt

Data_current-voltage.txt

Data_power input.txt

Data_power output.txt.

1. LSC device parameters and optical losses

A number of additional parameters may provide insight into potential loss mechanisms in LSCs. The performance of an LSC can be further quantified based on the concentration factor C , which provides a measure of the ability of the LSC to concentrate incident light to its edges. When C is larger than 1, the increased photon flux exiting the edges of the LSC lightguide leads to enhanced photocurrent generated by the attached PV cells compared to the situation where the PV is directly exposed to sunlight. C is defined as the product of the external photon efficiency of the LSC, η_{ext} , and its geometric gain G :

$$C = G\eta_{ext}$$

G is a parameter that accounts for the influence of the dimensions of the LSC. For planar devices, G is defined as:

$$G = \frac{A_{top}}{A_{edge}}$$

with A_{top} and A_{edge} being the area of the top surface of the LSC and the area of the edges where solar cells are placed, respectively.

η_{ext} is affected by several optical losses that depend on both the luminophore and the lightguide. The influence of such losses on η_{ext} can be described in terms of the efficiency η_i of each optical process i occurring in the LSC upon illumination.

Luminophore-related loss modes include: non-absorption of incident photons (η_{abs}); reabsorption of emitted photons by neighbouring optical centres (η_{self}); non-unity photoluminescence quantum yield (η_{PLQY}).

Lightguide-related loss modes include: surface reflection of incident photons (η_{surf}); photoluminescence not trapped within the lightguide (η_{trap}); parasitic absorption of waveguided photons by the lightguide and scattering of photons during transport due to imperfections or optical defects at the lightguide surface (η_{WG}).

These efficiencies can be practically estimated by adopting the following experimental approaches.

Luminophore-related loss modes

Loss mode (efficiency)	Contribution to η_{ext}	Experimental determination
Non-absorption of incoming photons (η_{abs}).	Fraction of incident light that can be absorbed by the LSC.	<p>The absorption spectrum $A(\lambda)$ of the LSC and the spectrum of the illumination source (S_{SO}, typically a solar simulator) are measured spectroscopically and used in:</p> $\eta_{abs} = \frac{\int_{\lambda_1}^{\lambda_2} S_{SO}(\lambda)(1-10^{-A(\lambda)})d\lambda}{\int_{\lambda_1}^{\lambda_2} S_{SO}(\lambda)d\lambda}$ <p>to give a numerical value that is dependent on luminophore concentration. The integration limits λ_1 and λ_2 are to be selected so as to account for the spectral breadth of the luminophore and the emission range of the light source.</p>
Reabsorption of emitted photons by neighbouring optical centres (η_{self}).	Fraction of photoluminescence photons not undergoing self-absorption losses.	<p>Scale the measured edge-emission spectrum of the LSC under full illumination to match the true reabsorption-free emission spectrum $S_{true}(\lambda)$ of the luminophore in the long wavelength region. The scaled edge-emission spectrum $S'_{edge}(\lambda)$ and $S_{true}(\lambda)$ are used in:</p> $\eta_{self} = \frac{\int_0^{\infty} S'_{edge}(\lambda)d\lambda}{\int_0^{\infty} S_{true}(\lambda)d\lambda}$ <p>to give a numerical value that is dependent on luminophore concentration. $S_{true}(\lambda)$ can be obtained by fluorescence measurements on a diluted solution of the luminophore, where no self-absorption occurs.</p>
Non-unity photoluminescence quantum yield (η_{PLQY}).	Fraction of emitted photons vs. absorbed photons.	<p>Standard procedure for measuring luminescence quantum yield ($PLQY_{obs}$) of solid samples using an integrating sphere, including a correction factor (a) that accounts for reabsorption/remission processes occurring in optically-thick samples:</p> $PLQY = \frac{PLQY_{obs}}{1 - a + a \cdot PLQY_{obs}}$ <p>with</p> $1 - a = \frac{\int_0^{\infty} S'_{obs}(\lambda)d\lambda}{\int_0^{\infty} S_{true}(\lambda)d\lambda}$ <p>in which $S'_{obs}(\lambda)$ is the front emission spectrum scaled to match $S_{true}(\lambda)$ in the long wavelength region.^{S1}</p>

Lightguide-related loss modes

Loss mode (efficiency)	Contribution to η_{ext}	Experimental determination
Surface reflection of photons incident on the lightguide (η_{surf}).	Fraction of incident light that is not reflected at the LSC surface; R is the specular reflectance at the surface of the lightguide material.	$\eta_{surf} = 1-R$, where R can be either calculated via the Fresnel law for specular reflection by knowing the refractive index n_{LSC} of the lightguide material ($R = (n_{LSC} - 1)^2 / (n_{LSC} + 1)^2$) or can be directly obtained through specular reflectance measurements with a conventional UV-vis apparatus equipped with an integrating sphere.
Photoluminescence emission leaving the lightguide via the escape cone (η_{trap}).	Fraction of isotropically emitted photons trapped within the lightguide by total internal reflection.	It can be calculated as first approximation based on the refractive index n_{LSC} of the lightguide material as $\eta_{trap} = \sqrt{1 - \left(\frac{n_{air}}{n_{LSC}}\right)^2}$ with n_{air} being the refractive index of the LSC surrounding medium (air, $n_{air} \approx 1$). This equation is not completely accurate for dichroic emitters. ^{S2,S3,S4}
Parasitic absorption of waveguided photons and photon scattering during transport due to imperfections or optical defects at the lightguide surface (η_{WG}).	Fraction of photoluminescence photons transported to the edges of the LSC without encountering matrix absorption, scattering centers, and incomplete TIR due to surface roughness.	The edge-emitted optical power of the LSC is collected by means of an integrating sphere upon spot illumination of the LSC slab with monochromatic light at increasing distances d from the collection edge and in the absence of self-absorption ($\eta_{self} = 1$, namely the emission wavelength of the monochromatic light should be selected not to fall within the absorption window of the luminophore). The decreasing exponential fit of the integrated edge-emitted optical power plotted versus d provides the attenuation length μ of the LSC. μ can be correlated to η_{WG} based on considerations related to the geometry of the lightguide. ^{S5,S6}

2. Example calculations of key LSC metrics

Herein, we demonstrate a typical procedure used to measure and report the key figures-of-merit needed to characterize the optical performance of LSC systems, as described in the main text and summarized in the checklist presented in Table 1: internal photon efficiency η_{int} , external photon efficiency η_{ext} and device efficiency η_{dev} . The data used in this section have been obtained through measurements acquired by the authors in the Department of Materials Science & Metallurgy of the University of Cambridge (UK) and in the Department of Chemistry, Materials and Chemical Engineering “Giulio Natta” of Politecnico di Milano (Italy). For reference, such data have been attached in supplementary files to this article. The experimental set up and the materials used in these measurements are described in a previous work by the authors.^{S7}

Evaluation of internal photon efficiency η_{int} and external photon efficiency η_{ext}

A square LSC device is placed on a black absorbing background and is illuminated by means of a calibrated solar simulator (AM 1.5G) with 1 Sun ($1000 \pm 10 \text{ W m}^{-2}$) irradiance. The optical power output at each edge of the LSC is directed towards the input port of an integrating sphere, where it is collected and directed to a fiber-optic-coupled calibrated spectroradiometer. The spectrally-resolved edge output photon count is collected from the spectroradiometer and calibrated into optical power (W).

The internal photon efficiency η_{int} and the external photon efficiency η_{ext} can be obtained from the experimental data using the following equations (as reported in the main text):

$$\eta_{int} = \frac{N_{ph-out}}{N_{ph-abs}} = \frac{\sum_{i=1}^{i=n} \int_{\lambda_1}^{\lambda_2} P_{out,i}(\lambda) \frac{\lambda}{hc} d\lambda}{\int_{\lambda_1}^{\lambda_2} P_{abs}(\lambda) \frac{\lambda}{hc} d\lambda} = \frac{\sum_{i=1}^{i=n} \int_{\lambda_1}^{\lambda_2} P_{out,i}(\lambda) \frac{\lambda}{hc} d\lambda}{\int_{\lambda_1}^{\lambda_2} P_{in}(\lambda) (1-10^{-A(\lambda)}) \frac{\lambda}{hc} d\lambda} \quad (S1)$$

$$\eta_{ext} = \frac{N_{ph-out}}{N_{ph-in}} = \frac{\sum_{i=1}^{i=n} \int_{\lambda_1}^{\lambda_2} P_{out,i}(\lambda) \frac{\lambda}{hc} d\lambda}{\int_{\lambda_1}^{\lambda_2} P_{in}(\lambda) \frac{\lambda}{hc} d\lambda} \quad (S2)$$

where N_{ph-in} is the total number of photons incident on the top surface of the LSC, N_{ph-out} is the total number of edge-emitted photons summed over all LSC edges (four in the case of a square LSC, thus $i = 1-4$) and N_{ph-abs} is the total number of photons absorbed by the LSC.

- N_{ph-in} is obtained from the input power spectrum $P_{in}(\lambda)$ of the light source incident on the illuminated surface area of the LSC (units for $P_{in}(\lambda)$: $\text{W m}^{-2} \text{ nm}^{-1}$).
- N_{ph-out} is obtained from the sum of the output power spectra $P_{out,i}(\lambda)$ measured for each edge of the LSC, considering the illuminated LSC surface as the reference area (units for $P_{out,i}(\lambda)$: $\text{W m}^{-2} \text{ nm}^{-1}$).
- N_{ph-abs} is obtained from the absorbed input power spectrum $P_{abs}(\lambda)$, by convolution of the absorption spectrum $A(\lambda)$ of the LSC and $P_{in}(\lambda)$.

In the expressions above, n is the number of LSC edges, λ is the wavelength of photons (in nm), h is Planck's constant (in J s), c is the speed of light (in nm s^{-1}).

The measured and calculated power and photon flux spectra are reported in the following.

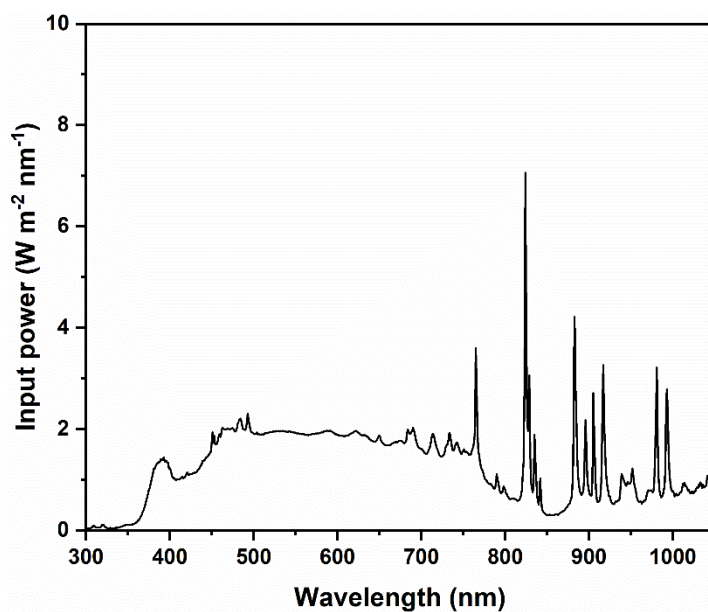


Figure S1. Input power of the light source incident on the illuminated surface area of the LSC, $P_{in}(\lambda)$.

Integration of the $P_{in}(\lambda)$ spectrum reported in Figure S1 between $\lambda_1 = 300$ nm and $\lambda_2 = 1050$ nm gives an integrated P_{in} of 960 W m^{-2} .

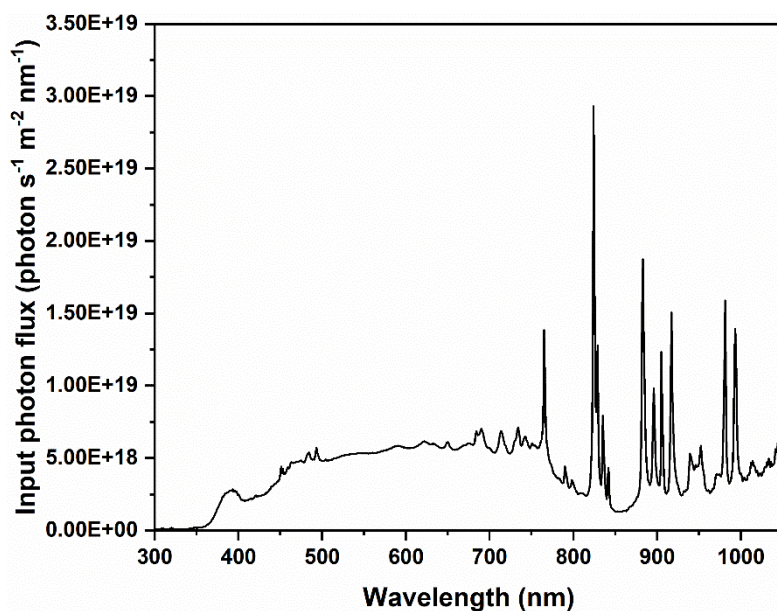


Figure S2. Input photon flux of the light source incident on the illuminated surface area of the LSC, $N_{ph-in}(\lambda)$.

Integration of the $N_{ph-in}(\lambda)$ spectrum reported in Figure S2 between $\lambda_1 = 300$ nm and $\lambda_2 = 1050$ nm gives an integrated N_{ph-in} of $3.23 \cdot 10^{21}$ photons $\text{s}^{-1} \text{m}^{-2}$.

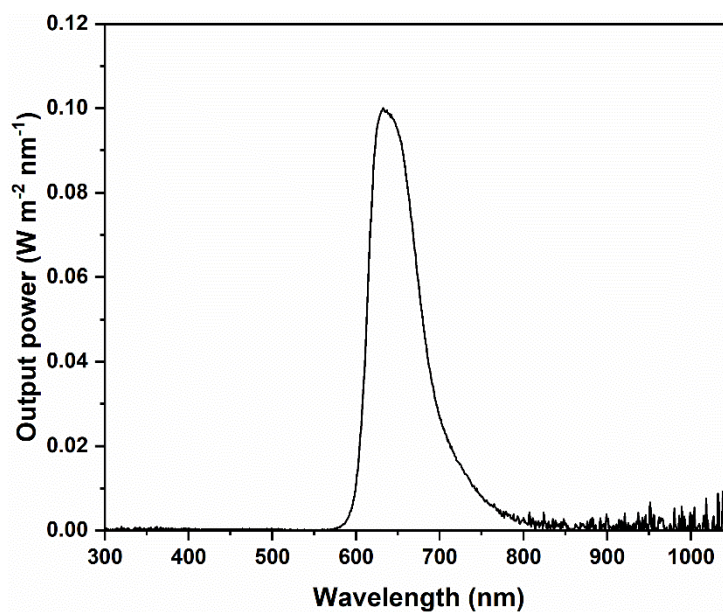


Figure S3. Output power measured for a single edge of the LSC, $P_{out,1}(\lambda)$.

Integration of the $P_{out,1}(\lambda)$ spectrum reported in Figure S3 between $\lambda_1 = 300$ nm and $\lambda_2 = 1050$ nm gives an integrated $P_{out,1}$ of 8.2 W m^{-2} . This value represents the optical power exiting one edge of the LSC.

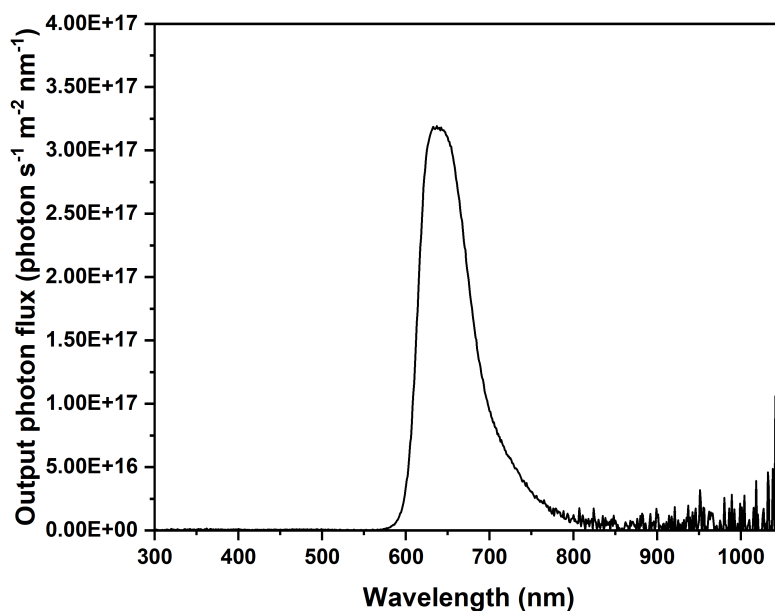


Figure S4. Output photon flux measured for a single edge of the LSC, $N_{ph-out,1}(\lambda)$.

Integration of the $N_{ph-out,1}(\lambda)$ spectrum reported in Figure S4 between $\lambda_1 = 300$ nm and $\lambda_2 = 1050$ nm gives an integrated $N_{ph-out,1}$ of $2.76 \cdot 10^{19}$ photons $\text{s}^{-1} \text{ m}^{-2}$. This value represents the photon flux exiting one edge of the LSC.

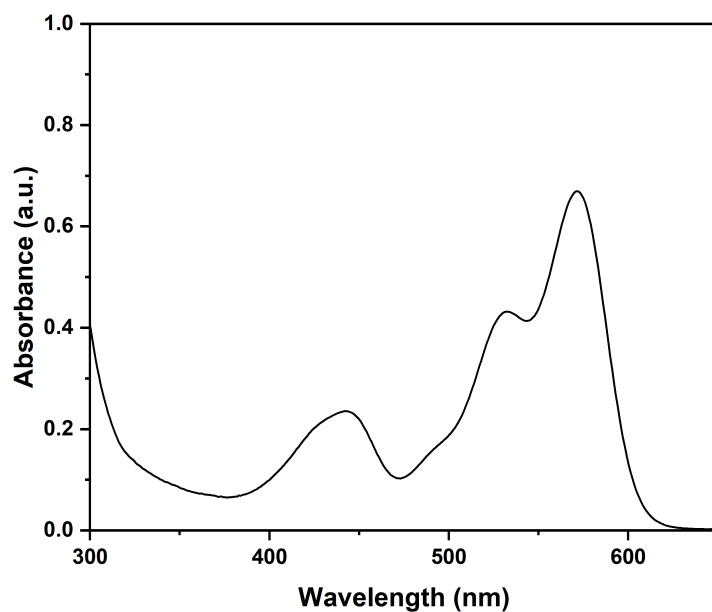


Figure S5. Absorption spectrum of the LSC, $A(\lambda)$.

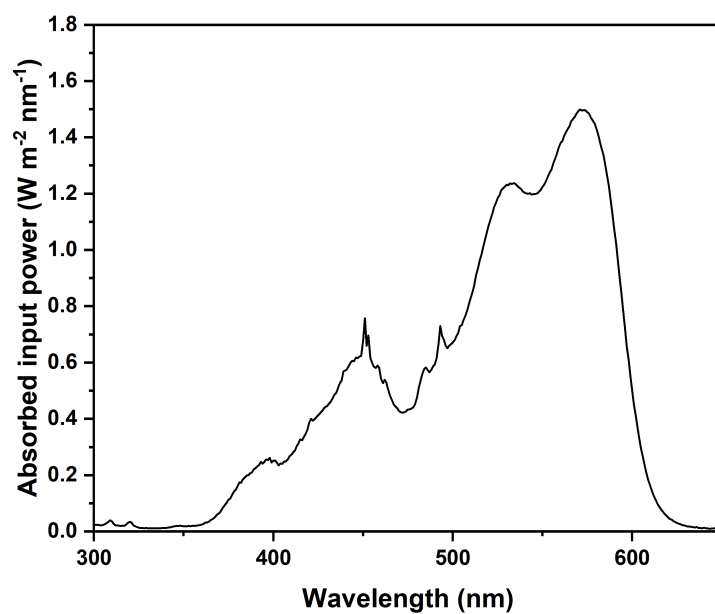


Figure S6. Input optical power absorbed by the LSC, $P_{abs}(\lambda)$.

Integration of the $P_{abs}(\lambda)$ spectrum reported in Figure S6 between $\lambda_1 = 300$ nm and $\lambda_2 = 1050$ nm gives an integrated P_{abs} of 176 W m^{-2} . This value represents the fraction of optical power incident on the LSC top area absorbed by the LSC.

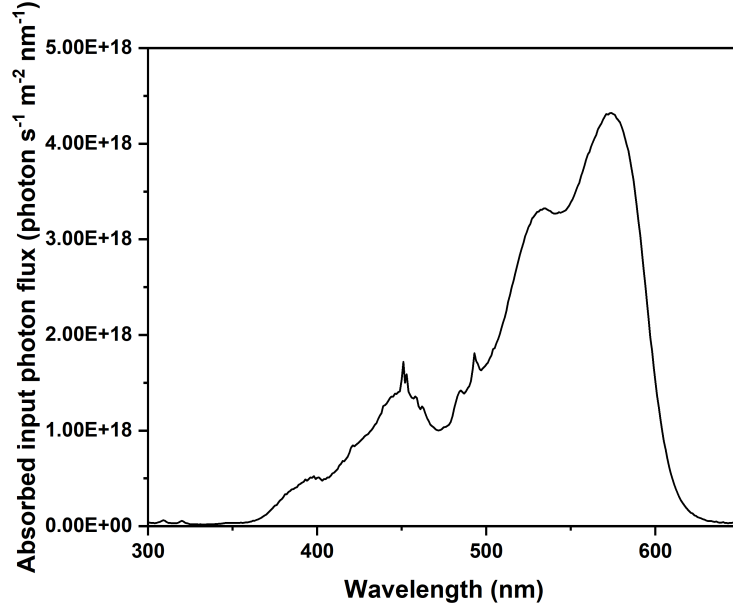


Figure S7. Input photon flux absorbed by the LSC, $N_{ph-abs}(\lambda)$.

Integration of the $N_{ph-abs}(\lambda)$ spectrum between $\lambda_1 = 300$ nm and $\lambda_2 = 1050$ nm gives an integrated N_{ph-abs} of $4.61 \cdot 10^{20}$ photons $s^{-1} m^{-2}$. This value represents the fraction of photon flux incident on the LSC top area absorbed by the LSC.

Based on the data reported in Figures S1-S7, the following single-edge efficiency values can be computed:

$$\eta_{int,1} = \frac{N_{ph-out,1}}{N_{ph-abs}} = \frac{2.76 \cdot 10^{19}}{4.61 \cdot 10^{20}} = 0.0599 \rightarrow \eta_{int,1} = 5.99\% \quad (S3)$$

$$\eta_{ext,1} = \frac{N_{ph-out,1}}{N_{ph-in}} = \frac{2.76 \cdot 10^{19}}{3.23 \cdot 10^{21}} = 0.00854 \rightarrow \eta_{ext,1} = 0.854\% \quad (S4)$$

Thus, considering a square LSC, the total efficiency values can be computed as follows:

$$\eta_{int} = 4 \cdot \eta_{int,1} = 0.2396 \rightarrow \eta_{int} = 23.96\% \quad (S5)$$

$$\eta_{ext} = 4 \cdot \eta_{ext,1} = 0.0342 \rightarrow \eta_{ext} = 3.42\% \quad (S6)$$

Evaluation of device efficiency η_{dev}

A $5 \times 5 \text{ cm}^2$ square LSC device is edge-coupled to four c-Si PV cells connected in series using an ethylene-vinyl acetate adhesive. The LSC-PV assembly is placed on a black absorbing background and is illuminated with a calibrated solar simulator (AM 1.5G) with 1 Sun ($1000 \pm 10 \text{ W m}^{-2}$) irradiance, preventing direct illumination of the edge-mounted PVs with a suitable black mask.

The performance of the assembled LSC-PV system is evaluated by recording the current-voltage curve under illumination and by calculating the device efficiency η_{dev} , defined as (see main text):

$$\eta_{dev} = \frac{\text{power from edge-coupled PV cell}}{\text{incident optical power on LSC surface}} = \frac{FF I_{SC} V_{OC}}{P_{in} A_{top}} \quad (S7)$$

where A_{top} is the active (top) surface area (m^2) of the LSC device, P_{in} is the incident solar-simulated power density (units: W m^{-2}) and FF , I_{SC} and V_{OC} are the fill factor (-), the short-circuit current (A) and the open-circuit voltage (V) of the edge-coupled PV cells, respectively.

The measured current-voltage curve and associated PV parameters are reported in the following.

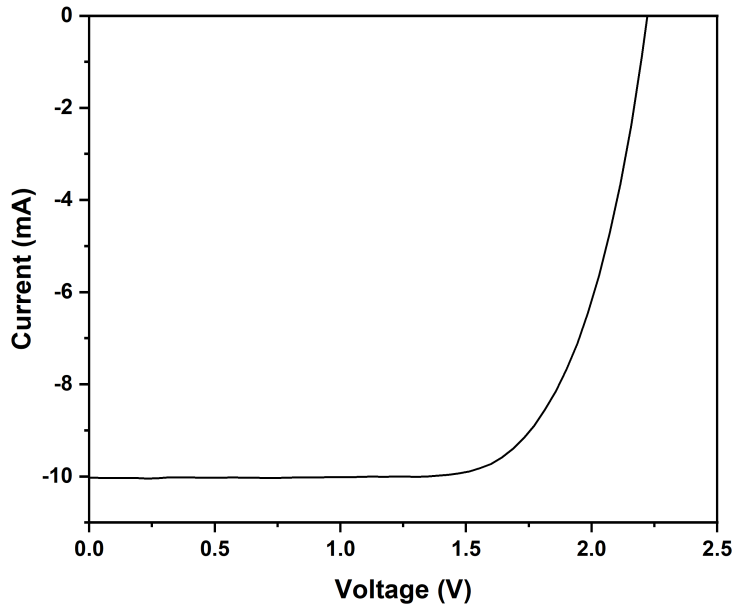


Figure S8. Characteristic current-voltage curve.

Based on the plot shown in Figure S8, the PV parameters can be extracted, to ultimately compute the value for η_{dev} :

$$\eta_{dev} = \frac{FF I_{SC} V_{OC}}{P_{in} A_{top}} = \frac{0.71 \cdot (10.03 \cdot 10^{-3}) \cdot 2.23}{960 \cdot (25 \cdot 10^{-4})} = 0.0066 \rightarrow \eta_{dev} = 0.66\% \quad (S8)$$

Supplementary references

- S1. Ahn, T.-S., Al-Kaysi, R. O., Müller, A. M., Wentz, K. M. & Bardeen, C. J. Self-absorption correction for solid-state photoluminescence quantum yields obtained from integrating sphere measurements. *Rev. Sci. Instrum.* **78**, 086105 (2007).
- S2. Verbunt, P. P. C., Sánchez-Somolinos, C., Broer, D. J. & Debije, M. G. Anisotropic light emissions in luminescent solar concentrators–isotropic systems. *Opt. Express* **21**, A485-A493 (2013).
- S3. Verbunt, P. P. C., de Jong, T. M., de Boer, D. K. G., Broer, D. J. & Debije, M. G. . Anisotropic light emission from aligned luminophores. *Eur. Phys. J. Appl. Phys.* **67**, 10201 (2014).
- S4. Mateen, F., Oh, H., Kang, J., Lee, S. Y. & Hong, S.-K. Improvement in the performance of luminescent solar concentrator using array of cylindrical optical fibers. *Renewable Energy* **138**, 691-696 (2019).
- S5. Erickson, C. S. *et al.* Zero-reabsorption doped-nanocrystal luminescent solar concentrators. *ACS Nano* **8**, 3461-3467 (2014).
- S6. Wiegman, J. W. E. & van der Kolk, E. Building integrated thin film luminescent solar concentrators: Detailed efficiency characterization and light transport modelling. *Sol. Energy Mater. Sol. Cells* **103**, 41-47 (2012).
- S7. Tatsi, E. *et al.* Thermoresponsive Host Polymer Matrix for Self-Healing Luminescent Solar Concentrators. *ACS Appl. Energy Mater.* **3**, 1152-1160 (2020).